J. Fluid Mech. (2020), *vol.* 895, A3.

doi:10.1017/jfm.2020.232

The nature of boiling during rewetting of surfaces at temperatures exceeding the thermodynamic limit for water superheat

C. F. Gomez[1,†], C. W. M. van der Geld[1], J. G. M. Kuerten[1], R. Liew[2], M. Bsibsi[2] and B. P. M. van Esch[1]

[1]Eindhoven University of Technology, P.O. Box 513, 5600 MB Eindhoven, The Netherlands

[2]Tata Steel Nederland Technology B.V., Postbus 10.000, 1970 CA IJmuiden, The Netherlands

(Received 3 October 2019; revised 12 February 2020; accepted 17 March 2020)

Rewetting is the establishment of water–surface contact that occurs during quenching of high temperature surfaces by water jet impingement. Rewetting is an unexpectedly complex phenomenon that has been reported to occur at surface temperatures significantly higher than the superheating limit of water. The presence of intermittently wet and dry episodes, and in particular the occurrence of so-called explosive boiling, is one of the theories to explain the contact of water with high temperature surfaces. However, there is a lack of experimental data in the literature to prove the presence of explosive boiling and intermittent wetting due to the small duration and scale of the rewetting phenomenon. In this study, recordings of the jet stagnation zone during rewetting are provided at a frame rate of 81 kfps. The high-speed recordings show a flashing regime consisting of intermittent (dry) bubble-rich and (wet) bubble-free periods at frequencies up to 40 kHz when the rewetted surface temperature exceeds the water superheat limit. As far as the authors know, these are the first direct observations of intermittent dry–wet periods occurring in the jet stagnation zone during quenching by water jet impingement. The dependency of the flashing frequency on initial surface temperature is quantified. A correlation between the size of the rewetting patch and the flashing frequency is found. Finally, a hypothesis to explain the role of water subcooling in maintaining the water–surface contact at surface temperatures well above the superheating limit of water is presented.

Key words: jets, boiling, condensation/evaporation

1. Introduction

1.1. *Background and aim*

Water jet impingement is widely used as a quenching technique in industry due to its high cooling potential. Controlled quenching is used in steel industry in the so-called run out table (ROT), where hundreds of water jet arrays impinge on a moving

† Email address for correspondence: camilagomez101191@gmail.com

steel slab. The steel slabs are cooled from approximately 900 °C to the final coiling temperature, which varies between 700 and 150 °C depending on the steel grade. The steel temperature evolution defines the final microstructure and mechanical properties, and therefore the ROT is a key stage in the production process.

The establishment of water–surface contact, also referred to as rewetting, is one of the most crucial and complex phenomena occurring during quenching by water jet impingement. This contact can occur immediately after impingement or after a film boiling period, depending on the process conditions. In any case, rewetting leads to a sharp increase of the surface heat flux due to its promotion of vigorous boiling activity. Although an increase of heat flux may seem desirable, uncontrolled rewetting can lead to several process complications. In metallurgy, uneven surface rewetting may lead to accumulation of thermal stresses, deformations, non-homogeneous mechanical properties and technical difficulties (Zhou *et al.* 2007; Fujimoto *et al.* 2016).

Experimental studies have reported rewetting to occur during subcooled water jet impingement at surface temperatures up to 900 °C (Ishigai, Nakanishi & Ochi 1978; Hatta, Kokado & Hanasaki 1983; Wang, Yu & Cai 2012). Rewetting at such elevated temperatures implies the ability of water to maintain contact with a surface at temperatures significantly higher than its thermodynamic limit of superheat. The thermodynamic limit of superheat of water (TLS, or thermodynamic limit for homogeneous nucleation) is 302 °C (Avedisian 1985). The TLS is the highest temperature that pure liquid water can sustain in a superheated metastable state at atmospheric pressure. Above this limit, the superheated liquid suffers instantaneous vaporization, also called explosive boiling. Assuming the veracity of the experimental studies reporting rewetting temperatures up to 900 °C, the mechanism by which liquid water contacts surfaces at such elevated temperatures is not yet understood.

Quenching of surfaces at temperatures above the TLS has been studied by Monde's group. In an experimental study, Woodfield, Monde & Mozumder (2005) observed chaotic water behaviour during the first stages of quenching. During this period, they report strong noise generation and delay of the wetting front movement. Stable water–surface contact during this period could not be confirmed by direct visualization, but intermittent contact was assumed given the noise and the order of magnitude of surface heat flux. The occurrence of explosive boiling followed by liquid deflection was assumed, leading to intermittent wet–dry periods (Islam *et al.* 2008). Given the time scale and location, direct observations or frequency measurements to confirm this assumption were not possible. Numerical studies allowed for the estimation of the explosive boiling time scale and limiting surface temperature, as well as the effect of material properties, in a single contact scenario (Hasan, Monde & Mitsutake 2011*b*,*c*).

The presence of intermittent dry and wet periods during pool and jet boiling has been speculated for a long time, based on boiling curve interpretations (Witte & Lienhard 1982), optical probe void fraction measurements (Bogdanic, Auracher & Ziegler 2009), numerical modelling (Seiler-Marie, Seiler & Simonin 2004) and sound recordings (Woodfield *et al.* 2005). The frequency of this phenomenon has been reported to be of the order of 2000 to 20 000 Hz (Seiler-Marie *et al.* 2004; Bogdanic *et al.* 2009). Temperature measurements with sensors located inside the test plate cannot record surface temperature fluctuations at such elevated frequencies and surface sensors are likely to modify the boiling and flow patterns. Direct observations during rewetting have been reported by Leocadio, van der Geld & Passos (2017), providing high-speed recordings of the subcooled jet stagnation zone by means of a borescope. Leocadio *et al.* (2017) observed a short period of stable film boiling at

initial surface temperatures above 450 °C of the order of milliseconds. Their work focuses on the effect of surface defects as rewetting promotors, the generation of air and vapour bubbles and a hypothesis where surface defects pierce the vapour–liquid interface and initiate the rewetting process. As far as the authors know, direct observations of intermittent dry and wet periods or explosive boiling occurring during quenching by water jet impingement have never been reported.

In industry, the water jet temperature is always below the water saturation temperature (subcooled water). The presence of subcooled water in the bulk is an expected added complexity when studying quenching. As pointed by Hall, Incropera & Viskanta (2001), subcooled water rewetting is likely to be hydrodynamically different from rewetting in pool boiling or saturated jets. In addition, the bubble dynamics may be affected by the presence of subcooled water. Parker & Granick (2014), for example, studied bubble behaviour during pool boiling with subcooled bulk water. Their study reported special behaviour in up to 10 % of the observed bubbles, including exploding, imploding or mushroom cloud bubbles.

Understanding the triggering and development of rewetting during quenching by subcooled water jet impingement is a necessity in order to improve the industrial process reliability and avoid economical losses. A comprehensive mechanism for rewetting above the thermodynamic limit of water superheat including experimental observations is yet to be described.

In the present study, we provide visual information regarding rewetting triggering and propagation in the stagnation zone during subcooled water jet quenching. The phenomena occurring in the initial stages of quenching are recorded at 81 kfps by using the high-speed visualization technique developed by Leocadio *et al.* (2017). Using this technique, we capture for the first time the presence of cyclic explosive boiling when rewetting occurs in smooth and sandblasted surfaces above 300 °C, leading to intermittent wet–dry periods. The dependency of the intermittent contact frequency on initial surface temperature and the area of the affected region will be examined and we will propose a mechanism for subcooled water contact with surfaces at temperatures above the TLS.

1.2. *Definitions*

Some quenching concepts have received multiple names in the literature, which might lead to confusion. For that reason, the definitions employed in this manuscript are summarized below:

(i) *Impingement*: instant when the tip of the water jet reaches the test plate surface.
(ii) *Stagnation zone*: area of the test plate directly underneath the circular water jet nozzle.
(iii) *Rewetting*: establishment of water–surface contact. If rewetting occurs simultaneously over the complete stagnation zone, a single rewetting moment is defined. If multiple rewetting patches appear, the rewetting moment of each patch is defined as the moment when that particular patch was first visible.
(iv) *Delay to rewetting*: time span between impingement and rewetting. If film boiling occurs, the delay to rewetting is equal to the duration of the film boiling regime. In the case of the absence of a film boiling regime, the delay to rewetting is equal to zero.
(v) *Flashing (boiling regime)*: highly unsteady boiling regime, more fully described in § 3 of this paper.

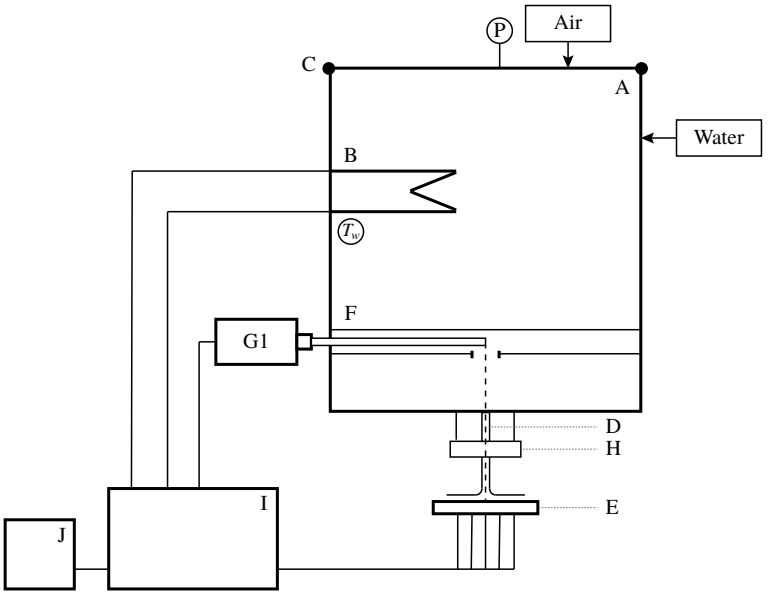

FIGURE 1. Quenching set-up schematic. A: Water tank. B: Water heater. C: Load cells (water flow measurement by tank weight change). D: Pneumatic valve and jet nozzle. E: Test plate. F: Borescope in tubing. G1: High-speed camera (stagnation zone view). H: LED illumination ring. I: Electrical box. J: PC for triggering and data acquisition.

(vi) *Delay to first flash*: time span between rewetting and the first boiling intermittency or flash of the flashing boiling regime.

(vii) *Thermodynamic limit of superheat (TLS)*: highest temperature that pure liquid water can sustain in a superheated metastable state at atmospheric pressure. Above this limit, the superheated liquid suffers instantaneous vaporization, also called explosive boiling.

(viii) *Leidenfrost temperature*: surface temperature above which a droplet develops a vapour cushion that isolates it from surface contact.

2. Methodology

The set-up used to perform the quenching experiments is shown in figure 1. The main component is a demineralized water tank (A), which can be heated by an electrical heater (B) or pressurized by compressed air injection. The water level is measured by three load cells (C) installed at 120° from each other around the tank. A circular nozzle (D) is screwed to the tank base. The water jet impingement onto the hot steel plate (E) is triggered by opening a pneumatic valve.

In this particular case, the water jet was driven by gravity and the water temperature was kept at 25 °C. The nozzle diameter is 9 mm and it is located at 3.6 cm from the plate surface, leading to a jet speed of 3.1 m s^{-1}.

The test plates were made from stainless steel AISI 316 with dimensions 50 × 50 × 10 mm. A single K-type thermocouple was located in the centre of the plate at 1 mm below the test plate surface, for the sole purpose of measuring the initial plate temperature. The test plate was heated by a portable resistance oven to the desired temperature. The heating time was kept below 1 h to avoid surface damage by oxidation, leading to a maximum test plate temperature of 650 °C.

Test plates with different surface finishes were used to study the effect of surface topology on rewetting. Three different test plates were used: a mirror-like smooth plate, a sandblasted rough plate and a plate with half-smooth and half-rough surface. The roughness was analysed by confocal optical profilometry at $\times 5$ magnification (Sensofar Plμ). The mirror-like surface was achieved first by sandpaper polishing and subsequently cloth polishing with 3 μm diamond particle spray, resulting in an average roughness of 300 nm. The sandblasted surface was machined in a sandblasting machine, resulting in a surface with an average roughness of 5 μm with peaks at a maximum height of 17 μm. The half–half surface was firstly polished, and later sandblasted while shielding half of the surface from the sanding.

The events occurring in the jet stagnation zone during the first instants of quenching were recorded at high speed by use of a fixed borescope (figure 1, F), installed in a tube that traverses the water tank and has a viewing window right above the jet stagnation zone. The borescope was type R080-028-090-10 from Olympus, with a working length of 280 mm and focal distance of 80 mm. The recordings were made using a high-speed camera (figure 1, G1) model Photron SA-X2 at 81 000 fps with resolution 512 $\times$ 272. The recording is triggered when the pneumatic valve is opened.

The main recording limitations are the spatial resolution and the frame rate. Given the spatial resolution, objects smaller than 0.1 mm and/or with blurry edges are difficult to discern. This could limit the observation of small bubbles or rewetting incipient spots. The recording frame rate and recording length are limited by the internal memory of the high-speed camera. We selected the recording settings that allowed us to observe the complete rewetting process with the maximum frame rate possible, resulting in a recording time of 87 ms at a frame rate of 81 kfps. The recordings provide discretized information in the form of video frames, meaning that any perturbation of frequency exceeding 40.5 kHz will not be perceived correctly.

3. Rewetting recordings

In this section, the high-speed recordings corresponding to the initial stages of quenching of surfaces at 650 °C when using a circular water jet at 25 °C are presented. Given the strong differences, sandblasted and smooth surface recordings are described separately.

The boiling regimes observed in the high-speed recordings are depicted using snapshots. These snapshots have been selected to illustrate the events seen in the recordings as clearly as possible. The complete rewetting recordings are attached to the online version of this paper as supplementary movies 1–4, available at https://doi.org/10.1017/jfm.2020.232. The images consist of a circle that corresponds to the jet stagnation zone (9 mm diameter) as seen from above.

3.1. *Sandblasted surface*

Rewetting recordings on sandblasted surfaces show immediate rewetting and vigorous boiling activity, even before the jet has developed over the complete stagnation zone. This vigorous boiling activity lasts for 45 ms after jet impingement on a plate with initial temperature of 650 °C. The initial vigorous boiling regime could be wrongly assumed to be chaotic if the recordings are played at high playback speed. When examining the recordings frame by frame, a pattern is perceived.

Figure 2 shows snapshots during a total period of 0.56 ms, showing consecutive bubble-rich and bubble-less periods alternating at high frequency. Sudden bubble generation occurs over the whole stagnation zone (figure 2*a*). In the following

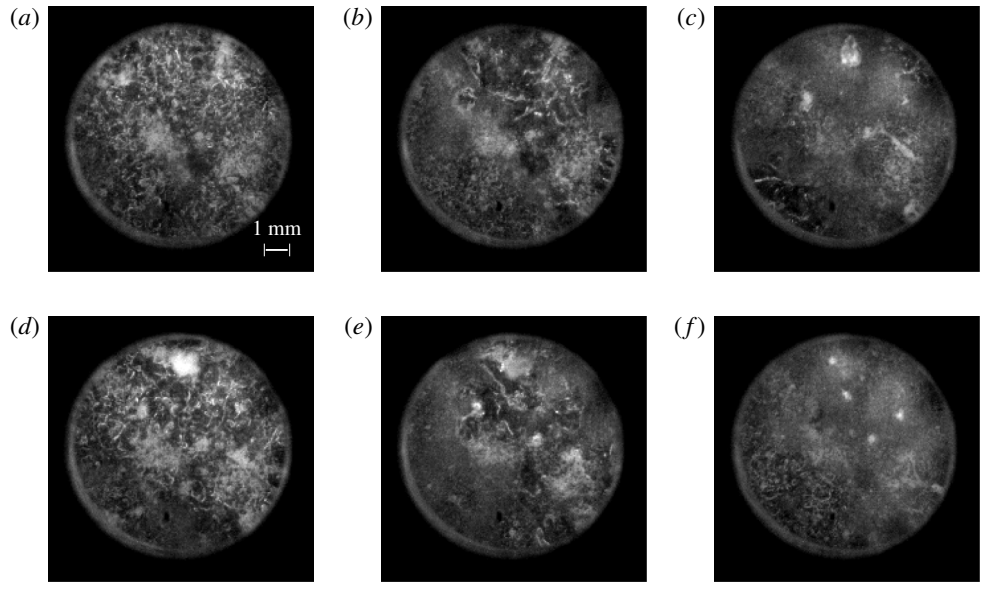

FIGURE 2. Rewetting during sandblasted plate quenching; initial plate temperature of 650 °C and water jet at 25 °C. Flashing regime. The circle corresponds to the 9 mm diameter stagnation zone. Time after impingement: (*a*) 9.931 ms; (*b*) 10.111 ms; (*c*) 10.214 ms; (*d*) 10.308 ms; (*e*) 10.456 ms; (*f*) 10.493 ms.

frames, all the bubbles collapse (figures 2*b* and 2*c*). After collapse, the surface is left bubble-less for a certain period of time before new bubbles suddenly nucleate (figure 2*d*). As observed before in figure 2(*b*), all the bubbles collapse (figure 2*e*) leading to a new bubble-less period (figure 2*f*). Both bubble generation and bubble collapse occur synchronously over the complete stagnation zone. This repetitive behaviour is observed as a flashing pattern in the recordings, with intermittent dark bubble-less periods and bright bubble-rich periods. This is most clearly seen if the movies are played at very low playback speed.

When flashing ceases after 45 ms (for initial surface temperature of 650 °C), boiling occurs in a particular manner (figure 3). Big bubbles are observed with long life times, of the order of 2–6 ms (figure 3*a–g*). These bubbles are much bigger than nucleate boiling bubbles. The big bubbles usually coalesce, sometimes growing to occupy the complete stagnation zone (9 mm diameter) before collapsing. During bubble growth, boiling activity is not observed inside the bubble, indicating that the surface in the bubble foot is dry. After collapse of the big bubbles with long life time, flashing is observed in the surface previously occupied by the bubble foot (figure 3*g–i*), indicating reheating of the surface during the bubble growth period.

Both the flashing boiling regime and the big bubble regime are unstable boiling regimes that do not correspond to film boiling or a normal nucleate boiling regime. These regimes could correspond to different stages of a regime comparable to the transition boiling observed in classical pool boiling. The existence of two different stages with intermittent contact and big bubbles agrees with the boiling curve interpretations by Witte & Lienhard (1982) and is similar to the visualizations of the classical transition boiling regime by, for example, Gentile (1989).

When the big bubble regime ceases, stable generation of nucleation boiling bubbles is observed, with a maximum observed diameter of 0.2 mm and lifetime of 0.1 ms.

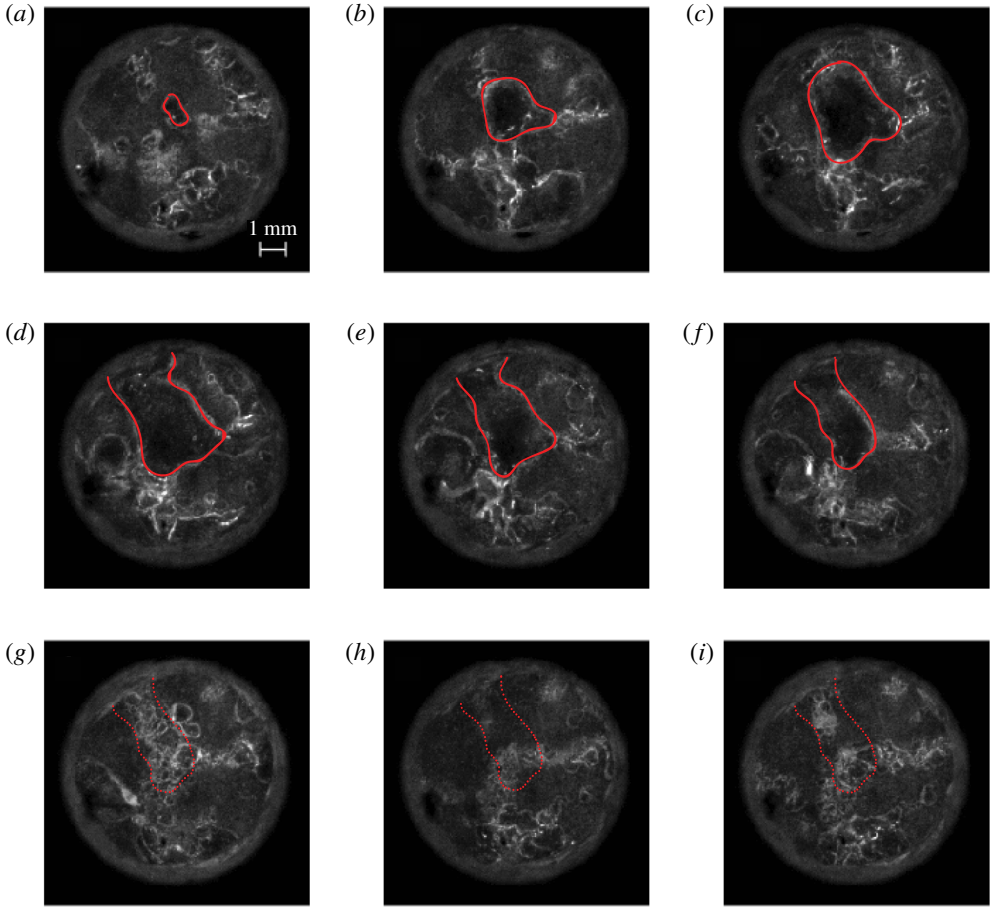

FIGURE 3. Rewetting during sandblasted plate quenching; initial plate temperature of 650 °C and water jet at 25 °C. Big bubble regime. The circle corresponds to the 9 mm diameter stagnation zone. The continuous red lines correspond to the visible bubble foot and the dotted lines correspond to the position of the collapsed bubble foot. Time after impingement: (*a*) 57.123 ms; (*b*) 58.086 ms; (*c*) 58.629 ms; (*d*) 59.296 ms; (*f*) 59.876 ms; (*g*) 60.370 ms; (*h*) 60.666 ms; (*i*) 60.802 ms.

Given the small size of these boiling bubbles and their low density, we suspect that the average bubble diameter in this case is too small to be observed in the recordings.

The observations reported in the above are typical for sandblasted surfaces with initial plate temperature in the range 300–650 °C. The complete recording of rewetting on a sandblasted surface and a detailed video of the flashing pattern are available on the online version of this paper as movie 1.

3.2. *Smooth surface*

Figure 4 corresponds to a series of snapshots taken from the high-speed recordings during the quenching process of a smooth plate at 650 °C. As reported before by Leocadio, van der Geld & Passos (2018), an initial film boiling period is observed (figure 4*a*). The film boiling regime is characterized by the presence of small moving

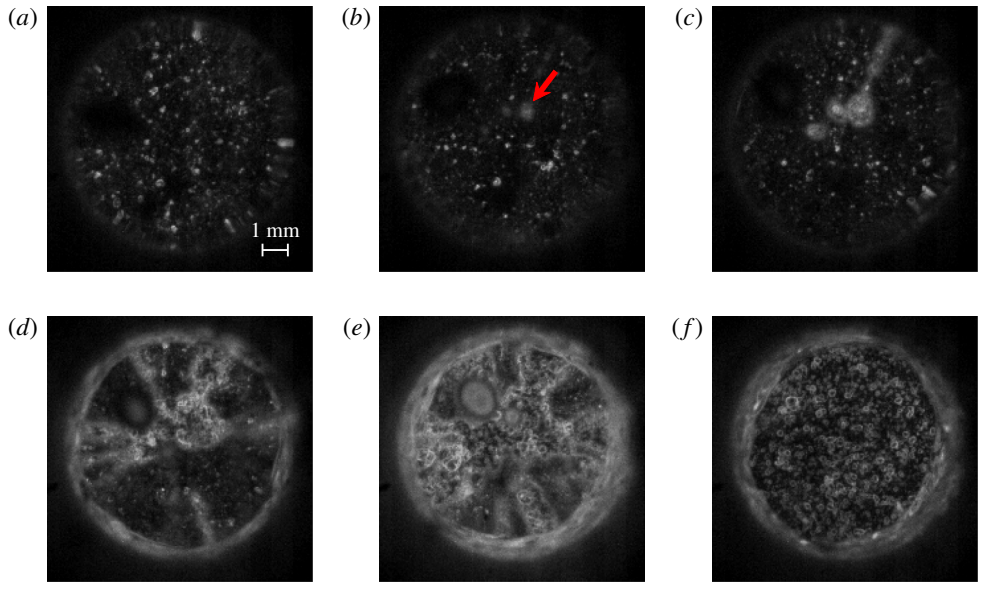

FIGURE 4. Rewetting during smooth plate quenching; initial plate temperature of 650 °C and water jet at 25 °C. The circle corresponds to the 9 mm diameter stagnation zone. Time after impingement: (*a*) 7.852 ms; (*b*) 19.555 ms; (*c*) 23.457 ms; (*d*) 31.617 ms; (*e*) 39.420 ms; (*f*) 63.185 ms.

white spots, which do not condense or coalesce. These objects have been reported to correspond to air bubbles at/near the vapour–liquid interface (Leocadio *et al.* 2017). We expect that these bubbles are degassing bubbles formed on dust particles in the heated liquid.

After 20 ms, a small bright area appears close to the centre of the stagnation zone (red arrow, figure 4*b*), indicating the start of a rewetting zone. As the bright area grows to show vigorous boiling activity in its interior, new bright areas appear in its surroundings (figure 4*c*). At some point in time, the different growing boiling areas merge (figure 4*d*,*e*) and occupy the complete stagnation zone (figure 4*f*).

The rewetting behaviour on smooth surfaces is significantly different from sandblasted surfaces. However, playing the smooth surface recordings frame by frame reveals the same flashing pattern as observed for sandblasted plates. Snapshots of bright bubble-rich and dark bubble-less periods in a smooth surface are presented in figure 5. When more than one wet patch appeared, flashing was observed in all the patches.

Flashing ceases after a certain time, before the complete surface is rewetted. When flashing in the wet patches ceases, stable nucleate boiling occurs. Nucleate bubbles in this case have a lifetime between 32.5 and 129.3 μs and maximum diameter of 0.6 mm. The density of nucleate bubbles in smooth surface recordings is significantly higher than in the sandblasted surface. For normal nucleate boiling and similar to our findings, Paz *et al.* (2015) reported smaller bubbles on rough surfaces than on smooth surfaces, which they attributed to the number of pores in the surface, their size and the modification of the contact angle. Similar findings were reported by Sisman *et al.* (2016).

The observations reported above are typical for smooth surfaces with initial plate temperature in the range 500–650 °C. The complete recording of rewetting on a

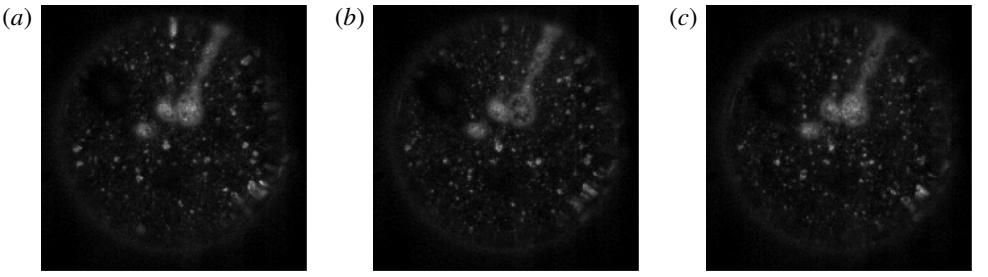

FIGURE 5. Flashing frequency on a smooth plate (see brightness changes in central patch); initial plate temperature of 650 °C and water jet at 25 °C. The circle corresponds to the 9 mm diameter stagnation zone. Time after impingement: (*a*) 23.284 ms; (*b*) 23.420 ms; (*c*) 23.469 ms.

smooth surface is available on the online version of this paper as movie 2, including a detailed video showing the flashing pattern in the small rewetting patches. At initial temperatures between 300 and 500 °C, the initial vapour film collapses prematurely in the complete stagnation zone and leads to flashing in the complete stagnation zone in a way comparable to the sandblasted surface recordings. A typical recording showing this behaviour is attached to the online version of this paper as supplementary movie 3.

3.3. *Half-smooth/Half-sandblasted surface*

In order to isolate the effect of surface finish from other factors like jet pressure instabilities or water temperature variations, a surface presenting both topologies was quenched under similar conditions (initial temperature 650 °C and water temperature 25 °C). Figure 6 shows representative snapshots of the rewetting phenomenon during that test. In the recordings, the left half of the stagnation zone corresponds to the sandblasted surface finish, while the right half corresponds to the smooth surface finish.

As can be seen, despite the proximity of both sections, each half shows the exact same behaviour as in the corresponding single topology test. On the left side, the sandblasted area shows flashing behaviour (figure 6*a–c*) followed by big transition boiling bubbles (figures 6*d* and 6*e*). On the right side, the smooth area shows film boiling (figure 6*a–c*) followed by small rewetting patches (figures 6*d* and 6*e*), initially flashing and later showing stable nucleate boiling bubbles.

Interestingly, around the time that the first rewetting patches appear on the smooth side, a wetting front is observed moving from the edge of the sandblasted area to the right smooth side (figures 6*d* and 6*e*). Given that rewetting occurs on the sandblasted side around 28 ms before rewetting on the smooth side, one could assume that in figure 6(*d*) the sandblasted side is cooler than the smooth side. In that case, the smooth surface in proximity to the sandblasted side could be cooled by internal conduction, leading to the wetting front movement. As time passes, the wet areas on the smooth side grow and occupy the complete recording zone. At that point, nucleate boiling is observed in the complete stagnation zone (figure 6*f*). Once again, the differences in mean bubble size between smooth and sandblasted areas are striking (figure 6*f*).

The complete recording of rewetting on the half-smooth/half-sandblasted plate is available on the online version of this paper as supplementary movie 4.

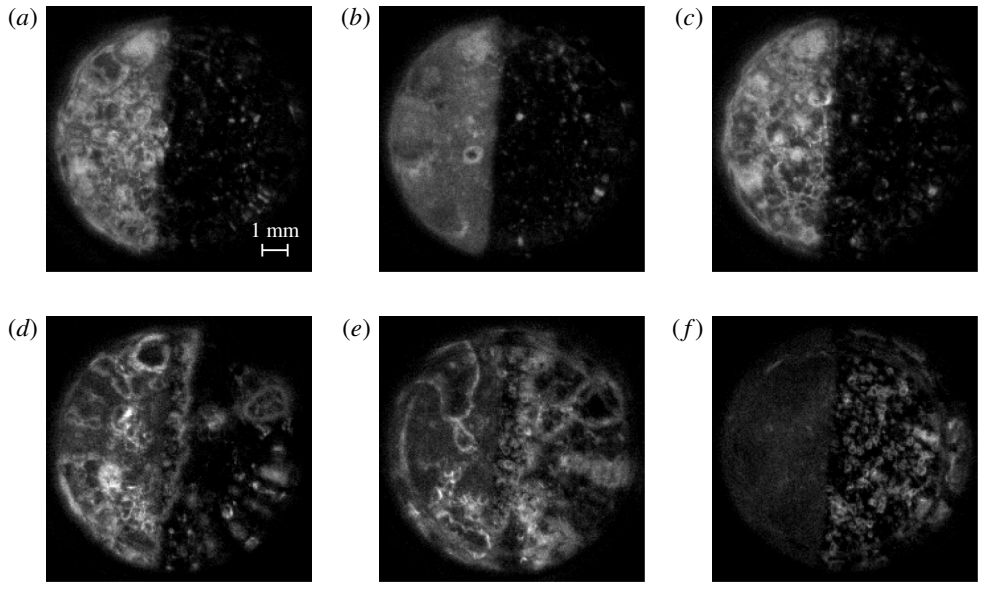

FIGURE 6. Rewetting during quenching of a half-sandblasted (left) and half-smooth (right) plate; initial plate temperature of 650 °C and water jet at 25 °C. The circle corresponds to the 9 mm diameter stagnation zone. Time after impingement: (*a*) 13.222 ms; (*b*) 13.333 ms; (*c*) 13.432 ms; (*d*) 33.445 ms; (*e*) 42.272 ms; (*f*) 68.370 ms.

4. Flashing behaviour analysis

A peculiar flashing behaviour has been observed during quenching of surfaces at up to 650 °C by subcooled water jet impingement at ambient pressure. In this section we clarify and analyse this phenomenon, including the effect of surface topology, initial surface temperature and length scale.

4.1. *Surface topology effect*

The high-speed recordings presented in § 3 show a flashing regime on both smooth and sandblasted surfaces. However, major differences regarding the rewetting incipience are observed between the two surface topologies. Quenching recordings on a half-smooth and half-sanded surface show that, at equal conditions, a smooth surface finish initially leads to a film boiling regime while a sandblasted surface finish triggers immediate rewetting and flashing. The surface topology apparently plays a major role in the rewetting temperature and rewetting mechanism.

In the past, the Leidenfrost temperature has been reported to be highly dependent on surface topology and surface wetting. Kim *et al.* (2011) reported an increase of the Leidenfrost temperature for highly porous surfaces, leading to immediate water–surface contact and violent boiling activity and without the expected film boiling regime. When a smooth surface was used under the same conditions, film boiling was observed before small liquid contact areas appeared. Bradfield (1966) reported the occurrence of some kind of explosive liquid–solid contact when pool quenching a highly porous graphite test piece. At equal conditions, smooth test pieces showed stable film boiling.

The studies mentioned above attribute the apparent decrease of the Leidenfrost temperature of porous surfaces with respect to smooth surfaces to their increased wettability. The relatively low wettability of a smooth surface leads to a stable vapour film. A porous, rough surface promotes water contact and we expect that, at sufficiently high surface temperature, this leads to water superheating and explosive boiling.

Although the rewetting and Leidenfrost temperatures do not share the same definition, they are related. Our direct recordings show similar behaviour as found by others in studies on the Leidenfrost effect. At similar surface and water temperature, smooth surfaces exhibit an initial film boiling period while sandblasted surfaces show immediate rewetting, as shown in § 3.

Our physical interpretation of this phenomenon is as follows. Liquid impinging on a rough surface has inertia that allows it to make contact with peaks on the surface. These peaks may, for example, result from artificial roughening of a surface (sandblasting). The contact depends on the angle of impact, but not on the temperature difference between liquid and surface. If the surface is rough enough for vapour (generated after or during contact) to escape sideways, contact between new liquid and the solid surface establishes even at surface temperatures exceeding the water superheat limit. As a result, a large amount vapour is generated in a short period of time (explosive boiling).

4.2. *Initial plate temperature effect*

Successive cycles of bubble-rich and bubble-less periods occur during flashing at a regular rate that will be named the flashing frequency in the following. In this section, the effect of initial plate temperature on the flashing frequency is presented for sandblasted and smooth surfaces. The flashing frequency is estimated based on the measured duration of 3 consecutive cycles. The duration of the cycles is counted by the number of frames between bubble-less periods. The maximum error in the duration of 3 consecutive cycles is equal to the time lapse between two consecutive frames (1/81 000 s). Therefore, the error bar for a frequency measurement of 40 kHz extends from 34 kHz to 48 kHz. The error bar for a frequency measurement of 1500 Hz extends from 1491 to 1509 Hz.

For sandblasted surfaces at initial temperatures above 300 °C, immediate rewetting is observed. Therefore, the delay to rewetting is equal to zero at all the studied temperatures, as shown in figure 7. A delay is observed between rewetting and the first flash of the flashing boiling regime, denominated here as delay to first flash. The delay to first flash decreases with increasing initial plate temperature, also shown in figure 7.

Figure 8 shows the effect of the initial surface temperature on the flashing frequency of sandblasted surfaces quenched by a water jet at 25 °C. Given that the delay to rewetting in these cases is zero, the delays observed in figure 8 correspond to the delay to first flash, also presented in figure 7 as empty squared markers. The flashing frequency is highest in the first cycles and decreases progressively until flashing ceases. Lower initial surface temperature leads to lower frequencies overall, as well as to shorter duration of the flashing regime. Flashing is not observed at surface temperatures below 300 °C, where stable nucleate boiling occurs immediately after impingement. This limit is of the order of the thermodynamic limit for water superheat (302 °C, Avedisian (1985)) and estimations of the surface temperature required for explosive boiling by Hasan *et al.* (2011*b*). The cycle duration measured from our

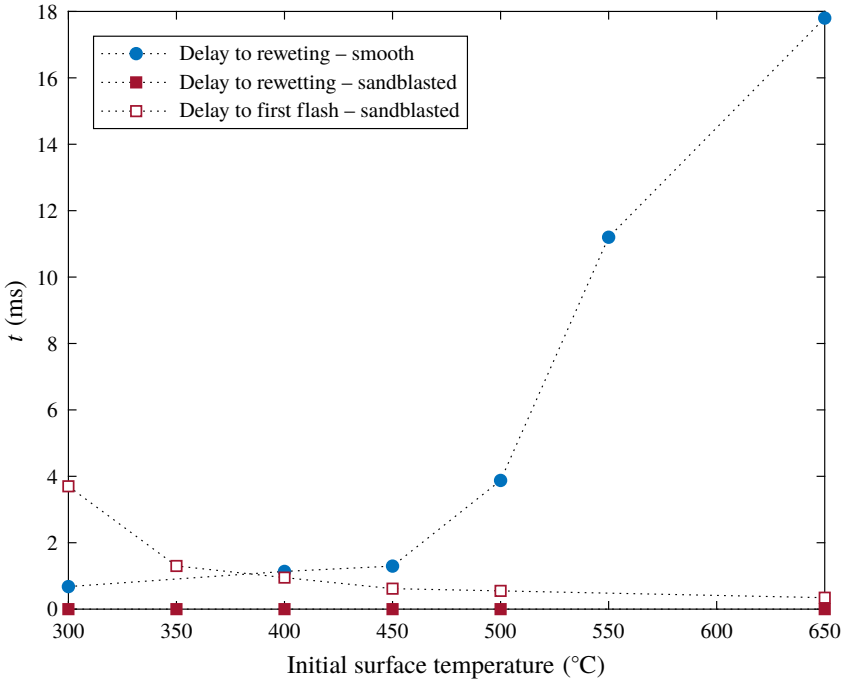

FIGURE 7. Delay to rewetting and delay to first flash at different initial temperatures for different surface topologies. The delay to first flash cannot be estimated in smooth surfaces due to the poor visibility of the small rewetting patches in the early stages of rewetting and the complexity of the non-homogeneous collapse of the vapour film.

recordings is significantly lower than the explosive boiling time scale calculated by Hasan *et al.* (2011*c*), which result from modelling a stagnant water film in a single contact scenario and do not include the bubble interaction with subcooled water. A complete intermittent contact boiling model including the effect of subcooled water (Seiler-Marie *et al.* 2004) resulted in frequencies of the same order of magnitude as our measurements. Bogdanic *et al.* (2009) also reported comparable intermittent contact frequencies resulting from optical probe measurements during water jet impingement boiling.

Peaks in the frequency history occur in the experiment with initial surface temperature equal to 650 °C and 500 °C (figure 8, circle and square markers, 7 and 14 ms after impingement). These peaks correspond to the stagnation zone being divided into 2 zones with unsynchronized flashing: for instance, one half of the stagnation zone is bubbly and the other half is bubble-less at the same time. The fact that the two zones are completely out of phase indicates that the different flashing zones behave as coupled oscillators affected by the water flow and bubble growth. In these cases, the frequency estimations are based on one of the two flashing areas. However, the frequencies of both areas are comparable. The frequency decreases as soon as the two flashing zones come in phase again and a single flashing zone is observed. The increase in frequency during asynchronous flashing in the stagnation zone can be related to a reduction of the length scale of the flashing area that results in increased frequency; this will be further examined in the next section.

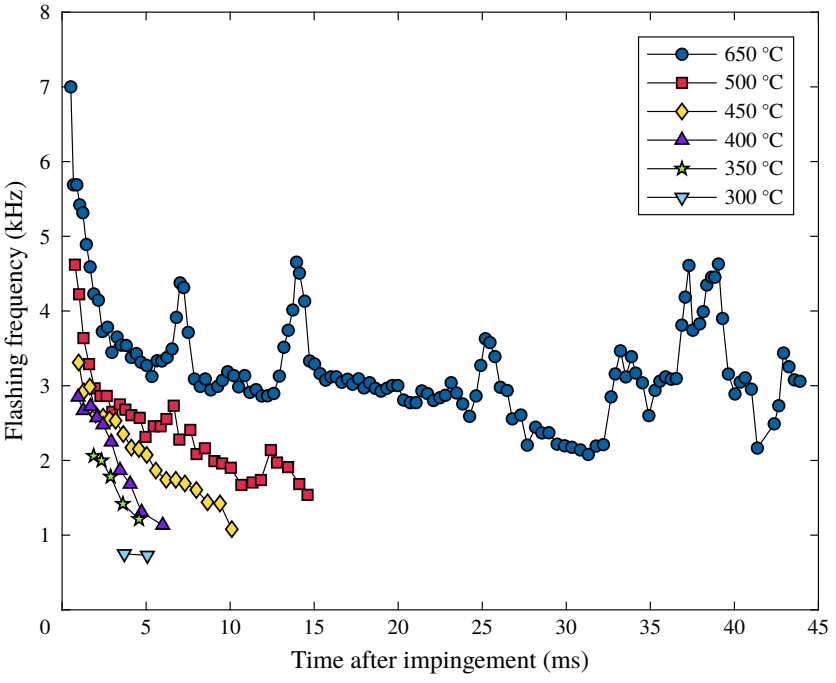

FIGURE 8. Flashing frequency histories measured on a sandblasted plate; water jet at 25 °C. The legend corresponds to the initial surface temperature.

On smooth surfaces at initial temperatures between 300 and 450 °C, stable film boiling does not occur. Only a premature and unstable vapour film is observed before multiple rewetting patches appear over the complete surface and a flashing regime develops similar to what was observed on a sandblasted surface. The premature vapour layer leads to a very short delay to rewetting in this temperature range (figure 7), which increases with initial plate temperature as the vapour layer thickens. In this range, the effect of initial plate temperature on the flashing frequency in smooth surfaces (figure 9) is comparable to the sandblasted experiments. Similar to sandblasted surfaces, there is absence of flashing at temperatures below 300 °C. Therefore, it is concluded that flashing occurs independently of the surface finish and only if the surface temperature is above the thermodynamic limit of superheat of water.

At initial temperatures above 450 °C, a stable film boiling regime occurs in smooth surfaces, which leads to differences compared to sandblasted surfaces. As can be observed in figure 7, the delay to rewetting in smooth surfaces, corresponding to the film boiling duration, significantly increases with temperature above 450 °C. This indicates that a longer cooling time is necessary to reach the rewetting temperature that allows the appearance of rewetting patches. After this period of stable film boiling, flashing is only observed inside small rewetting patches, as described in § 3.2. The frequency estimations in figure 9 show that flashing in small patches occurs at frequencies substantially higher than in other experiments where flashing occurs over the complete stagnation zone. The surface temperature alone is not likely to provide an explanation for the higher frequencies, since the sandblasted surfaces do not show this sudden frequency increase at similar initial temperatures. A possible explanation

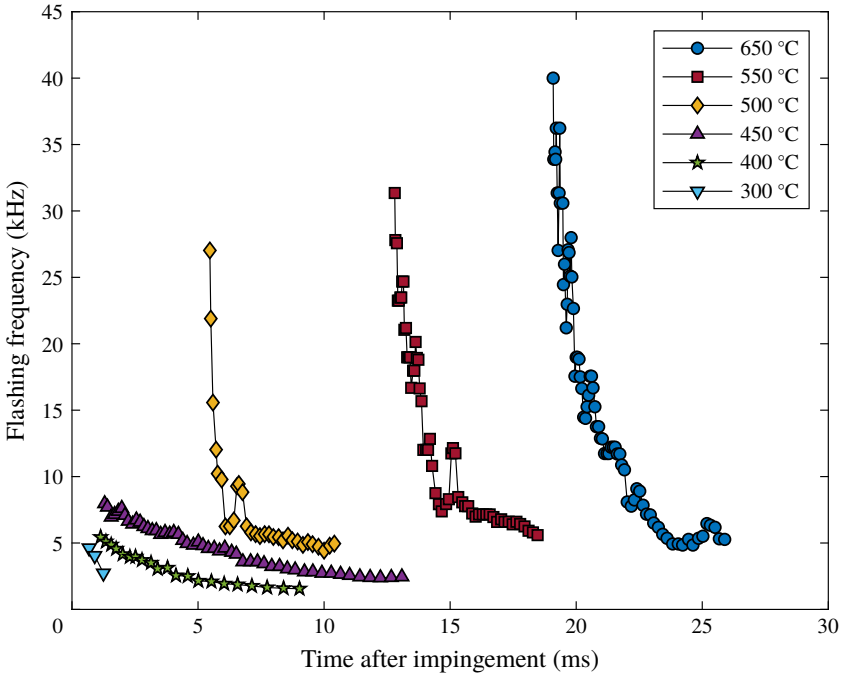

FIGURE 9. Flashing frequency histories measured on a smooth plate; water jet at 25 °C. The legend corresponds to the initial surface temperature.

is in the decrease of the length scale of the flashing area, which is further explored in the next section.

4.3. *Length scale effect*

In the previous section we presented two phenomena that might be explained by a dependency of the flashing frequency on the length scale of the flashing region. The first one is a boost in frequency by the occurrence of a second out-of-phase flashing region in the stagnation zone. The second one is the significantly higher flashing frequency in rewetting patches that are small as compared to complete stagnation zone.

The flashing area in sandblasted surfaces could extend beyond the observable stagnation zone, hindering an estimation of the length scale of the area where the flashes occur. Luckily, the size of the flashing patches in smooth plates after film boiling is limited, allowing measurement of the flashing patch area.

Estimations of flashing area, cycle duration and time after rewetting were therefore made in rewetting patches at different locations in the stagnation zone on smooth surfaces at initial plate temperatures of 500, 550 and 650 °C. The time since the patch emerged is the lapse of time since that particular patch was first visible in the recordings. The area of flashing patches was estimated assuming an elliptic shape and measuring the widths and lengths of the patches. Only flashing cycles with distinct and sharp edges of the patch were selected, to minimize the error in the size estimations. The total error in the diameter measurements is assumed to be of the order of the smallest visible object in the recordings (approximately 0.05 mm), resulting in the following typical measurements: 0.1 ± 0.03 and 1.3 ± 0.1 mm^2.

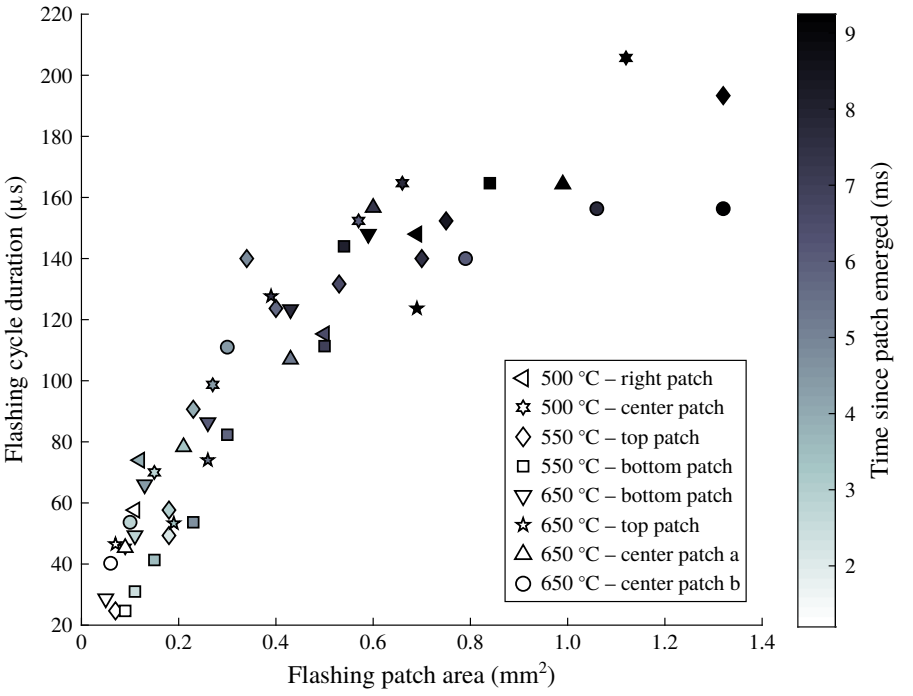

FIGURE 10. Flashing cycle duration vs rewetting patch area. The legend gives the initial surface temperature and an indication of the patch location in the stagnation zone. The marker colour indicates the lapse of time since that certain rewetting patch became visible in the recording (time since patch emerged), and the axes correspond to the patch area and flashing cycle duration at that particular moment.

Figure 10 shows the relationship between flashing patch area, flashing cycle duration and time since each patch emerged after film boiling in smooth surfaces. As pointed out before, length scale measurements in sandblasted surfaces and smooth surfaces below 500 °C are not possible because flashing could extend outside of the field of view.

The results show a correlation between flashing frequency and patch area, independent of patch location in the stagnation zone. The trend confirms the observations from the previous section that an increase in length scale leads to an increase of flashing cycle duration, i.e. a decrease in flashing frequency.

The fact that the cycle duration is independent of the patch location indicates that it does not depend on the pressure or speed variation along the stagnation zone. Another important conclusion from figure 10 is that patches of equal area always show the same flashing frequency at the same time since the patch emerged, independently of the initial plate temperature. This indicates that the rewetting patches always appear at the same surface temperature, i.e. the temperature that allows contact between wall and liquid, or rewetting temperature. The rewetting patch acts as a heat sink and, as times goes on, cooling of the surrounding surface by internal conduction leads to an outward movement of the wetting front and increase of the patch area.

A physical explanation of these data is presented in § 5.1.

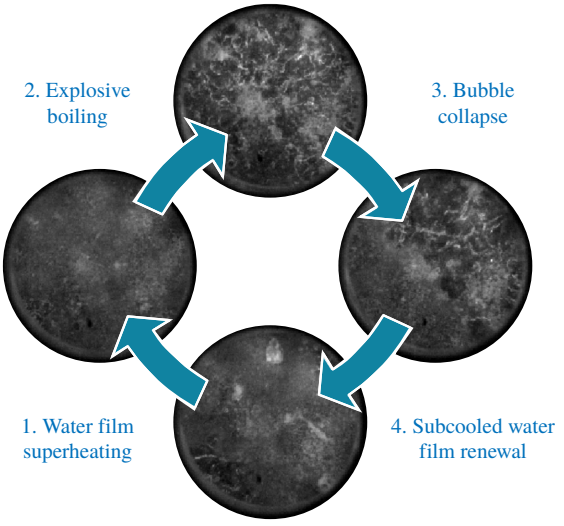

FIGURE 11. Liquid contact hypothesis: cyclic explosive boiling and condensation.

5. Flashing cycle

A big discussion in the field is the possibility of stable rewetting above the thermodynamic limit of water superheat (Woodfield *et al.* 2005; Islam *et al.* 2008; Hasan, Monde & Mitsutake 2011*a*; Hasan *et al.* 2011*b*,*c*). If stable rewetting occurs at such elevated temperatures, the question is by which mechanism liquid water is allowed to maintain contact with a surface above the superheating limit.

The high-speed recordings of the stagnation zone of § 3 indicate that water–surface contact occurs almost instantly at temperatures way above the thermodynamic limit of superheat. In cases where the initial surface temperature is above 300 °C, a unique and highly temperature dependent phenomenon is observed: successive bubble-rich and bubble-less periods corresponding to a highly dynamic flashing boiling regime.

Based on the direct observations presented in the previous sections, we propose the following hypothesis that relates this flashing boiling regime to water–surface contact at elevated temperatures. An explosive boiling cycle is proposed that consists of four stages (figure 11).

(i) *Water film superheating*: upon contact with a surface above the thermodynamic limit of superheat or TLS (302 °C, Avedisian (1985)), the temperature of the water film adjacent to the surface rapidly increases to above the saturation temperature into the superheated range.

(ii) *Explosive boiling*: when the water temperature reaches the TLS, the metastable superheated water undergoes a violent phase transition, named explosive boiling, to a more stable two-phase state. The explosive boiling phenomenon generates rapidly growing vapour bubbles.

(iii) *Bubble collapse*: once the vapour bubbles grow to be thicker than the superheated water film, contact with the bulk subcooled water occurs. The vapour bubbles collapse upon contact with the cold fluid (Parker & Granick 2014).

(iv) *Subcooled water film renewal*: the volume previously occupied by vapor bubbles is immediately filled with the impinging subcooled water. The subcooled water film absorbs heat from the hot plate surface, returning to stage (i) again and hence closing the cycle.

The energy required for vaporization is taken from the solid surface, whose temperature decreases. The cycle is stopped once the surface temperature is no longer high enough to elevate the water temperature above the TLS. From that moment onward, more regular types of boiling occur.

Our hypothesis explains the mechanism of rewetting at temperatures above the superheat limit. The continuous feeding of new subcooled water in the bulk is in essence the explanation for rewetting occurring at elevated surface temperatures. According to our hypothesis, dynamic water–surface contact at surface temperatures above the TLS is allowed by a cyclic explosive boiling activity, maintained by condensation of the vapour bubbles upon contact with continuously refreshed bulk subcooled water.

5.1. *Flashing cycle and length scale effect*

The study in § 4.3 shows that smaller flashing areas correspond to shorter flashing cycle duration, or higher flashing frequency. The edges of the small rewetting patches considered in § 4.3 are a limit for bubble growth during the flashing cycle. As a consequence, the area of the rewetting patch is considered to be the maximum bubble area. The smaller the patch area, the smaller is the maximum allowed bubble size, and the shorter the cycle duration. The rewetting patch acts as a heat sink, cooling the surrounding surface by internal conduction as time goes on. As a result, the patch size increases with time, the maximum allowed bubble size increases and so does the flashing cycle duration. When the complete stagnation zone is rewetted, the flashing zone length scale is equal to or bigger than the stagnation zone and therefore the limits of the flashing areas are usually not visible. In the few cases where two flashing zones are visible, the flashing cycles are completely out of phase and behaving as coupled oscillators. This observation is also in agreement with Seiler-Marie *et al.* (2004), which stated that if liquid contact occurs in one intermittent contact zone, vapour must be ejected in another nearby zone. Our observations indicate that synchronous flashing or the presence of a single flashing zone is the preferred situation in the stagnation zone, possibly as a consequence of the jet pressure distribution.

The data of figure 10 show two trends with increasing patch area. From 0 to approximately 0.4 mm^2 the cycle duration is proportional to the area. For higher values a levelling off can be seen, with possibly a linear dependency with a lower proportionality constant. Since the bubbles created in the flashing patch area grow nearly simultaneously, the combined interfaces of the bubbles are essentially the interface of a gas pocket with a typical area of the size of the flashing patch. It is well known that in the early stage of bubble growth the interfacial area is proportional with time (Plesset & Zwick 1954; van Ouwerkerk 1971; Baltis & van der Geld 2015). In this period, diffusion is the controlling mechanism, making the typical length scale proportional to the square root of time and the typical area proportional to time. The observation that the relation in figure 10 is linear up to approximately 0.4 mm^2 indicates that diffusion of heat is the controlling mechanism and that the generated vapour behaves collectively as a single bubble. The data are in quantitative agreement with the experimental data presented by Baltis & van der Geld (2015) for the growth of a single bubble: 0.2 mm^2 for 50 μs growth time, versus approximately 0.15 mm^2 for the same growth time in figure 10. Moreover, the linear relationship is in agreement with the following relation derived by van Ouwerkerk (1971):

$$R \propto Ja\sqrt{\alpha t}, \tag{5.1}$$

where R is the bubble radius, Ja is the Jakob number, t is the bubble growth time and α is the thermal diffusivity. The Jakob number is defined as $C_p(T_{wall} - T_{sat})/h_{vap}$, where C_p is the specific heat of the fluid, T_{wall} and T_{sat} are the surface and saturation temperatures, respectively, and h_{vap} is the enthalpy of vaporization. In this particular case, the relationship holds although T_{wall} varies with time as cooling occurs, similar to van Ouwerkerk (1971) and Baltis & van der Geld (2015).

For rewetting patches bigger than 0.4 mm^2, figure 10 shows a levelling off in the cycle duration. For a single bubble behaviour, the longer the time since the patch emerged, the lower the temperature at the wall has become, the smaller the Jakob number and the slower bubble growth should be. However, the levelling off in the cycle duration in figure 10 shows the contrary. This change of trend is likely to indicate that the vapour generated in patches bigger than 0.4 mm^2 no longer behaves as a single bubble, but instead as a group of several bubbles, each smaller than the patch.

The two different trends are also visible in figure 9 at temperatures equal or higher than 500 °C. An initial sharp frequency decrease is observed corresponding to the first regime, highly affected by the length scale of the patches, where the vapour behaves as a single bubble. In a second regime with more stable frequencies, the curves resemble those where flashing occurs over areas larger than the stagnation zone. As pointed out in § 4.3, length scale quantification is not possible if flashing occurs over the complete stagnation zone, since the flashing area may extend beyond the field of view of the borescope.

5.2. *Flashing cycle and initial temperature effect*

The effect of initial temperature on the flashing frequency (flashing over the complete zone in figures 8 and 9 below 500 °C) is also explained by the Jakob number relation by van Ouwerkerk (1971). A higher initial surface temperature corresponds to a higher driving temperature difference for bubble growth, $T_{wall} - T_{sat}$. The higher the temperature difference, the higher the Jakob number and the faster the bubble growth step. It is expected that the height of the effective vapour layer, probably consisting of several bubbles next to each other, increases during a single flash cycle. Henceforth, a smaller growth velocity leads to a longer time for bubble growth, a longer flashing cycle and a lower flashing frequency. The same argument holds for the decrease of flashing frequency over time; the longer the flashing regime has occurred, the lower the surface temperature and therefore the lower the frequency as well.

Regarding the delay to the first flash, sandblasted surfaces showed a decreasing delay for increasing initial plate temperature (figure 7). At higher initial temperature, shorter times are required for the subcooled water film to reach the superheated state and to suffer explosive boiling for the first time. This explains the first flash to occur earlier with increasing initial plate temperature.

6. Conclusions

The possibility of rewetting happening at surface temperatures above the TLS has been an important discussion in the field of quenching. Many have speculated on a possible explanation (Woodfield *et al.* 2005; Islam *et al.* 2008; Hasan *et al.* 2011*a*,*b*,*c*), but closure can only be found in direct optical observations under hardly accessible circumstances. The question by which mechanism liquid water is allowed to contact surfaces at such elevated temperatures has been answered in the present study with the aid of dedicated experiments. Using a stagnation zone visualization

technique, we provide high-speed recordings of rewetting of a subcooled water jet during quenching of both smooth and sandblasted surfaces. The recordings show the presence of intermittent and violent bubble generation at surface temperatures above the TLS. A hypothesis is presented that explains the mechanism by which rewetting occurs when quenching surfaces at elevated temperatures by subcooled water jet impingement. The following conclusions are drawn:

(i) At initial plate temperatures above the TLS a new and dynamic boiling regime is observed, consisting of cyclic violent bubble formation followed by bubble collapse. This regime has intermittent bubble-rich and bubble-less periods at frequencies up to 40 kHz. This so-called cyclic explosive boiling regime occurs independently of the surface topology. At higher initial plate temperature, the intermittency occurs at higher frequencies.

(ii) A clear relationship is found between the flashing cycle duration and the area of the flashing patch. For flashing areas smaller than 0.4 mm^2, the relationship indicates a diffusion controlled mechanism and single bubble behaviour.

(iii) According to our hypothesis, the subcooled water suffers superheating and subsequent rapid boiling at elevated surface temperature (above 300 °C). The violently growing bubbles contact the subcooled bulk water and collapse, allowing the refreshing of the subcooled water film. This cycle is repeated until the surface temperature is below the TLS.

Acknowledgements

This research was carried out under project number F41.5.14525 in the framework of the Partnership Program of the Materials innovation institute M2i (www.m2i.nl) and the Foundation of Fundamental Research on Matter (FOM) (www.fom.nl), which is part of the Netherlands Organization for Scientific Research (www.nwo.nl).

Declaration of interests

The authors report no conflict of interest.

Supplementary movies

Supplementary movies are available at https://doi.org/10.1017/jfm.2020.232.

REFERENCES

AVEDISIAN, C. T. 1985 The homogeneous nucleation limits of liquids. *J. Phys. Chem. Ref. Data* **14** (3), 695–729.

BALTIS, C. H. M. & VAN DER GELD, C. W. M. 2015 Heat transfer mechanisms of a vapour bubble growing at a wall in saturated upward flow. *J. Fluid Mech.* **771**, 264–302.

BOGDANIC, L., AURACHER, H. & ZIEGLER, F. 2009 Two-phase structure above hot surfaces in jet impingement boiling. *Heat Mass Transfer/Wärme- Stoffübertrag.* **45** (7), 1019–1028.

BRADFIELD, W. S. 1966 Liquid–solid contact in stable film boiling. *Ind. Engng Chem. Fundam.* **5** (2), 200–204.

FUJIMOTO, H., HAYASHI, N., NAKAHARA, J., MORISAWA, K., HAMA, T. & TAKUDA, H. 2016 Boiling heat transfer during impingement of two or three pipe laminar jets onto moving steel sheet. *ISIJ Intl* **56** (11), 2016–2021.

GENTILE, D. 1989 Les mécanismes de l'Ébullition, sfrs-cerimes, edf, https://www.canal-u.tv/video/cerimes/les_mecanismes_de_l_ebullition.13294.

HALL, D. E., INCROPERA, F. P. & VISKANTA, R. 2001 Jet impingement boiling from a circular free-surface jet during quenching: Part 2. Two-phase jet. *Trans. ASME J. Heat Transfer* **123** (October), 901–910.

HASAN, M. N., MONDE, M. & MITSUTAKE, Y. 2011*a* Homogeneous nucleation boiling during jet impingement quench of hot surfaces above thermodynamic limiting temperature. *Intl J. Heat Mass Transfer* **54** (13–14), 2837–2843.

HASAN, M. N., MONDE, M. & MITSUTAKE, Y. 2011*b* Lower limit of homogeneous nucleation boiling explosion for water. *Intl J. Heat Mass Transfer* **54** (15–16), 3226–3233.

HASAN, M. N., MONDE, M. & MITSUTAKE, Y. 2011*c* Model for boiling explosion during rapid liquid heating. *Intl J. Heat Mass Transfer* **54** (13–14), 2844–2853.

HATTA, N., KOKADO, J. & HANASAKI, K. 1983 Numerical analysis of cooling characteristics for water bar. *Trans. ISIJ* **23**, 555–564.

ISHIGAI, S., NAKANISHI, S. & OCHI, T. 1978 Boiling heat transfer for a plane water jet impinging on a hot surface. In *6th International Heat Transfer Conference*, vol. 1, pp. 445–450. Hemisphere Publishing Corporation Toronto, Canada.

ISLAM, M. A., MONDE, M., WOODFIELD, P. L. & MITSUTAKE, Y. 2008 Jet impingement quenching phenomena for hot surfaces well above the limiting temperature for solid–liquid contact. *Intl J. Heat Mass Transfer* **51** (5–6), 1226–1237.

KIM, H., TRUONG, B., BUONGIORNO, J. & HU, L. W. 2011 On the effect of surface roughness height, wettability, and nanoporosity on Leidenfrost phenomena. *Appl. Phys. Lett.* **98** (8), 1–4.

LEOCADIO, H., VAN DER GELD, C. W. M. & PASSOS, J. C. 2017 Degassing, boiling and rewetting in free surface jet quenching. In *9th. World Conference on Experimental Heat Transfer, Fluid Mechanics and Thermodynamics, Iguazu Falls, Brazil*.

LEOCADIO, H., VAN DER GELD, C. W. M. & PASSOS, J. C. 2018 Rewetting and boiling in jet impingement on high temperature steel surface. *Phys. Fluids* **30** (12), 122102.

VAN OUWERKERK, H. J. 1971 The rapid growth of a vapour bubble at a liquid–solid interface. *Intl J. Heat Mass Transfer* **14** (9), 1415–1431.

PARKER, S. & GRANICK, S. 2014 Unorthodox bubbles when boiling in cold water. *Phys. Rev.* E **89** (1), 1–9.

PAZ, C., CONDE, M., PORTEIRO, J. & CONCHEIRO, M. 2015 Effect of heating surface morphology on the size of bubbles during the subcooled flow boiling of water at low pressure. *Intl J. Heat Mass Transfer* **89**, 770–782.

PLESSET, M. S. & ZWICK, S. A. 1954 The growth of vapor bubbles in superheated liquids. *J. Appl. Phys.* **25** (4), 493–500.

SEILER-MARIE, N., SEILER, J. M. & SIMONIN, O. 2004 Transition boiling at jet impingement. *Intl J. Heat Mass Transfer* **47** (23), 5059–5070.

SISMAN, Y., SADAGHIANI, A. K., KHEDIR, K. R., BROZAK, M., KARABACAK, T. & KOSAR, A. 2016 Subcooled flow boiling over microstructured plates in rectangular minichannels. *Nanoscale Microscale Thermophys. Engng* **20** (3–4), 173–190.

WANG, H., YU, W. & CAI, Q. 2012 Experimental study of heat transfer coefficient on hot steel plate during water jet impingement cooling. *J. Mater. Process. Technol.* **212** (9), 1825–1831.

WITTE, L. C. & LIENHARD, J. H. 1982 On the existence of two 'transition' boiling curves. *Intl J. Heat Mass Transfer* **25** (6), 771–779.

WOODFIELD, P. L., MONDE, M. & MOZUMDER, A. K. 2005 Observations of high temperature impinging-jet boiling phenomena. *Intl J. Heat Mass Transfer* **48** (10), 2032–2041.

ZHOU, Z., LAM, Y., THOMSON, P. F. & YUEN, D. D. W. 2007 Numerical analysis of the flatness of thin, rolled steel strip on the runout table. *Proc. Inst. Mech. Engrs* **221** (2), 241–254.